Seasonal Marginal Growth on Otoliths of Seven Alaska Groundfish Species Support the Existence of Annual Patterns

Daniel K. Kimura, Delsa M. Anderl, and Betty J. Goetz

Reprinted from the Alaska Fishery Research Bulletin
Vol. 12 No. 2, Winter 2007
The Alaska Fisheries Research Bulletin can be found on the World Wide Web at URL:
http://www.adfg.state.ak.us/pubs/afrb/afrbhome.php

Alaska Fishery Research Bulletin 12(2):243–251. 2007.

Seasonal Marginal Growth on Otoliths of Seven Alaska Groundfish Species Support the Existence of Annual Patterns

Daniel K. Kimura, Delsa M. Anderl, and Betty J. Goetz

Abstract: The Alaska Fisheries Science Center's Age and Growth Program has been collecting qualitative otolith edge growth data for many of the principal species that it ages. The edge-type data collected are coded on a scale from 0 to 5, in an attempt to categorize the characteristics of the outermost growth zone of the otolith for the month of capture. Edge growth classification data can be subject to biases when age readers are looking for a particular pattern of growth. However, analysis of edge-type data can be used to determine the apparent strength and timing of seasonal growth patterns, and thus provides a weak form of age validation. We develop a simple model that allows us to estimate the signal strength and timing of otolith edge growth using standard nonlinear least squares. We do this by combining edge codes so that they are concentrated into two distinct categories: category 1 which represents an otolith with a full increment of opaque growth or a translucent zone on the edge (with perhaps a hint of new opaque growth), or category 3 which represents an otolith which has substantial growth, ¼ to ½ of the previous year's otolith growth, on its edge. Because the remaining categories (2 and 4) contained relatively few observations, categories 1 and 3 can be treated using a logit-like transformation, and then modeled with a cosine function. This model appeared to capture a strong seasonal trend in edge-type growth in 7 species for which reasonable amounts of data were available. These results support that the growth rings found in many Alaska groundfish are generally annual marks, but do not validate that conventional ages from otolith ring counts for any of these species are accurate.

INTRODUCTION

The Alaska Fisheries Science Center (AFSC) has a disciplined method of age determination (Kimura and Anderl 2005) that includes lead age readers who resolve questions of ageing criteria, precision testing to ensure repeatability of ageing criteria, and a radiometric age validation specialist who provides radiometric and C-14 age validations when feasible. Age data and edge-type data generated since about 1990 are readily available for study and examination.

Conventional age determination from otoliths is based on the assumption that a pattern of annual growth increments is present. In theory, opaque zones represent periods of rapid growth and higher calcification, whereas translucent zones represent periods of slower growth and low calcification (Pannella 1974; Chilton and Beamish 1982). Opaque and translucent bands appear respectively as dark and light zones under transmitted light, or as light and dark zones under reflected light. A seasonal pattern in otolith edge types can aid in the verification of the hypothesis that an annual ring (opaque/translucent zone pair) is laid down once per year. The determination of edge type, as described in this paper, is subjective. Therefore, Campana (2001) considered this "marginal increment analysis" to be one of the weakest forms of age validation.

The timing of the translucent zone deposition is of particular interest. By international convention, marine fish species are assumed to have a birth date of January 1, regardless of the actual hatch date (Chilton and Beamish 1982; Panfili et al. 2002). An age reader must therefore interpret edge growth as it relates to this January 1 birth date. When assigning an age, an age reader must attribute any apparent opaque edge growth to either the current growth year (not counted) or the past growth year (counted). This classification takes into account a number of other variables which affect interpretation, such as the date of collection, the general age range (old versus young), and the width of the growth increment in comparison to previous increments. For example, in an otolith collected in July, the reader may observe an opaque band on the edge equal in width to the previous year's opaque growth. The reader must judge whether this growth is attributable to the current growth (not counted) or whether this growth is attributable to the past year's growth cycle (counted). In most cases, this edge growth would not be counted. However, if the same pattern was observed

---

Authors: Daniel K. Kimura, Delsa M. Anderl, and Betty J. Goetz are with the Alaska Fisheries Science Center, National Marine Fisheries Service, NOAA, 7600 Sand Point Way NE, Seattle, WA 98115-6349. Email: Dan.Kimura@noaa.gov
Acknowledgements: We thank Beth Matta, Dan Cooper, and two anonymous reviewers for many constructive comments.

in February, the reader typically could assume that the translucent zone had not yet been deposited, the growth is attributed to the previous growth year, and this edge growth would be counted as an additional year of growth (i.e., the age estimate would equal the number of translucent bands plus one). This need to determine age using edge interpretations with reference to the international birth date, and documentation of translucent zone deposition timing is what motivated the Age and Growth Program at the AFSC to collect large amounts of data on edge type.

In this paper we attempt to capture the seasonal otolith edge growth patterns for 7 species (walleye pollock *Theragra chalcogramma*, sablefish *Anoplopoma fimbria*, Atka mackerel *Pleurogrammus monopterygius*, Pacific ocean perch *Sebastes alutus*, northern rockfish *Sebastes polyspinis*, yellowfin sole *Limanda aspera*, northern rocksole *Lepidopsetta polyxystra*) for which substantial amounts of edge growth data have been collected. We fit a cosine function to logit data that describes the strength and timing of the otolith edge growth patterns. Fitting this model to data allows statistical tests for the null hypothesis that there is no growth pattern, and a confidence interval for the time of year during which the "logit" peaks, roughly interpreted as when the opaque growth is completed or the translucent zone is deposited.

MATERIALS AND METHODS

Edge Code Definitions

For many years, AFSC age readers have been encouraged to record observations of edge type on their ageing forms, and enter these into a database. The otolith data analyzed here were aged between 1990 and 2005. The "standard data codes" (Table 1, column 1) are the documented codes which are the Ageing Program's standard definitions of edge type. These standard codes ranged from 0 to 5, and are the basic data usually recorded by age readers.

The "expanded data codes" (Table 1, column 2) are the result of some age readers attempting to classify those situations where edge type is difficult to determine but a range of data codes can be assigned (e.g., standard codes 1–2). In this paper, when edge

Table 1. Standard data codes are the documented codes for otolith edge interpretation at the AFSC. Expanded data codes are extensions of the standard data codes used by some age readers in an attempt to be more precise. Final category codes were calculated from Standard and Expanded codes and were the categories actually used in the analysis: (1) a full increment of opaque growth or a translucent zone on the edge (with perhaps a hint of new opaque growth), (2) slight opaque edge growth beyond the last translucent zone, (3) an opaque edge with ¼ to ½ the opaque growth of the previous opaque increment, and (4) an opaque edge with ½ to a full year's opaque growth on the edge.

Standard Data Codes		Expanded Data Codes		Final Category Codes
0:	Strong annulus on the edge (translucent zone)	0		1
		0.5:	halfway between standard data codes 0 and 1	1
1:	Strong annulus with halenation (slight halo of growth)	1.0		1
		1.5:	halfway between standard data codes 1 and 2	2
2:	Up to ¼ of marginal opaque growth as compared to previously deposited opaque zone.	2.0		3
		2.5:	halfway between standard data codes 2 and 3	3
3:	Up to ½ of marginal opaque growth as compared to previously deposited opaque zone.	3.0		3
		3.5:	halfway between standard data codes 3 and 4	4
4:	Full year of marginal opaque growth as compared to previously deposited opaque zone.	4.0		1
		4.5:	halfway between standard data codes 4 and 5	1
5:	Full year of marginal opaque growth with an annulus appearing to form along the otolith margins.	5.0		1
		5.5:	halfway between standard data codes 5 and 0	1

type was interpreted as a range of standard codes, say 1–2, we interpreted it as an expanded code of 1.5. In a sense these expanded codes are more precise than the "standard data codes" because they allow for twice as many categories, but at the same time these data are less definitive in terms of the category definitions.

"Final category codes" (Table 1, column 3) are conversions of the "standard data codes" and the "expanded data codes" into categories that are less ambiguous, and that are amenable to seasonal analysis, for the purpose of the analysis presented here. We categorized these data into 4 edge categories: (1) a full increment of opaque growth or a translucent zone on the edge (with perhaps a hint of new opaque growth), (2) slight opaque edge growth beyond the last translucent zone, (3) an opaque edge with ¼ to ½ the opaque growth of the previous opaque increment, and (4) an opaque edge with ½ to a full year's opaque growth on the edge.

Looking at the standard data codes, one might ask what happened to those otoliths having from ½ to a full year's opaque growth. Apparently this category is difficult to discern and age readers did not originally feel they needed this category when keeping tabs of qualitative edge growth data. This may be particularly true because otolith opaque zones typically become narrower at older ages. Final categories 2 and 4 are essentially ambiguous codes that are between standard data codes, and thus have fewer observations. These codes were essentially ignored in the analysis.

The remaining final categories 1 and 3 are fairly unambiguous and can be interpreted as follows. Category 1 includes those otoliths that have either a full year of opaque growth on the edge, followed perhaps by translucent growth, which might be followed by only a hint of opaque growth (described as halenation). Final category 3 includes those otoliths that have substantial opaque growth up to half of the previous year's growth increment.

Photographic Examples of Otolith Edge Type

The photographs presented in this paper are under reflected light which shows opaque zones as white and translucent zones as narrow and dark. Edge type can sometimes be determined from the surface of whole otoliths of young fish, as from the 3-year-old walleye pollock otoliths depicted in Figure 1, and assigned

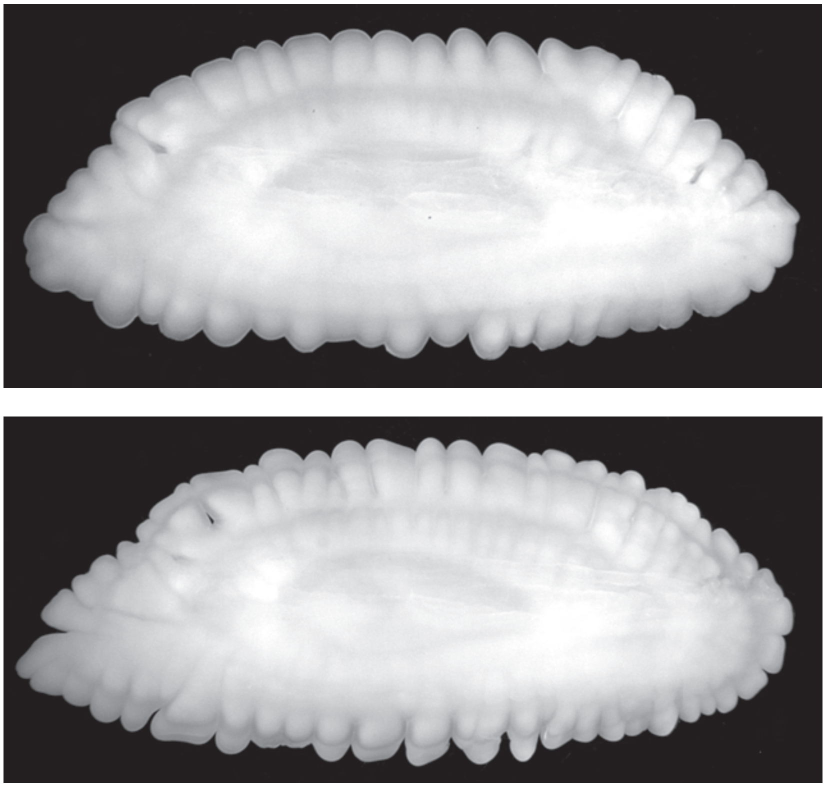

Figure 1. Photograph of two 3-year-old whole walleye pollock otoliths captured in the Bering Sea. Top otolith has final edge category 1, collected March 16, showing a full year's otolith growth (wide opaque zone) on the edge. Bottom otolith has final edge category 3, collected June 7, showing a partial year's otolith growth (narrow opaque zone) on the edge (see Table 1).

final edge categories 1 (top) and 3 (bottom). Note that the outermost zone is broad and white (Figure 1, top) and narrow and white (Figure 1, bottom).

Usually the edge type is determined from a cut-and-burn otolith cross section, such as this cross section from a 23-year-old yellowfin sole shown in Figure 2, and assigned a final edge category 3. Note that the outer opaque zone in Figure 2 is quite broad, and the time of year can itself suggest the edge type. This interpretation problem indicates why edge type provides only a very weak form of validating that growth rings are annual marks.

In contrast, an otolith cross section from a 5-year-old sablefish (Figure 3) has a translucent zone (narrow dark zone) right on the edge, and was assigned a final edge category of 1.

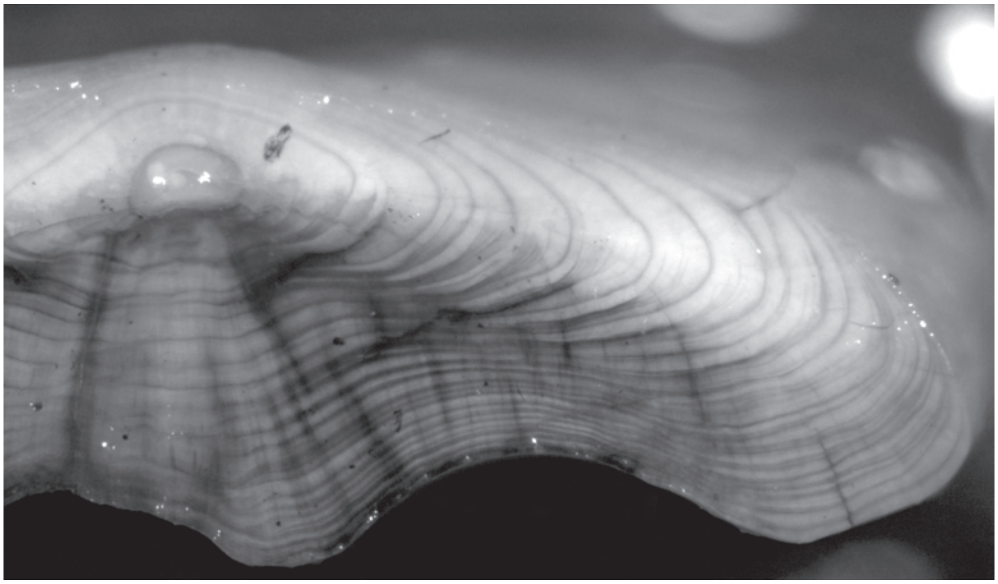

Figure 2. Cut-and-burnt otolith of a yellowfin sole collected on April 28 and aged 23 years. This otolith was given a final edge category of 3, with a partial year's growth (opaque zone) on the edge. However, it might be interpreted as a full year's growth if collected later in the year, illustrating the subjective nature of edge-type determinations.

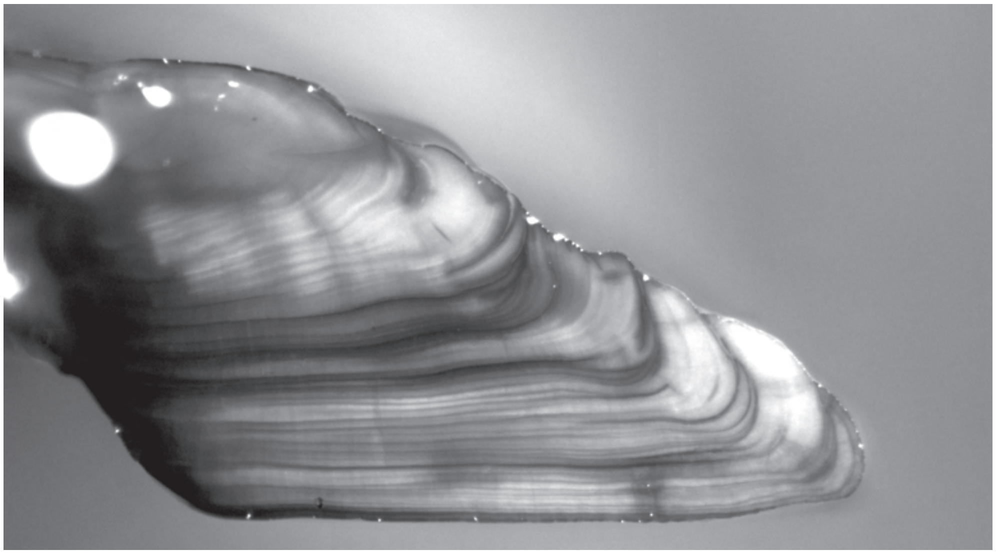

Figure 3. Cut-and-burnt otolith from a 5-year-old sablefish collected on June 2. This otolith was given a final edge category of 1, with a strong translucent zone (dark zone) occurring on the otolith edge.

Logit Model

We calculated the proportion of otoliths assigned to each final category code (1 through 4) for the month of collection j, as p_{1j}, p_{2j}, p_{3j} and p_{4j}. Results will later show that p_{2j} and p_{4j} were relatively small, and thus it followed that relative edge growth in each month could be modeled as: $y = \log(p_{1j}/p_{3j})$. By definition $\text{logit}(p) = \log(p/(1-p))$ (Bishop et al. 1975), so the (y_j) are nearly logits. To avoid an awkward terminology we will from now on refer to these "near logits" as "logits."

These logits, (y_j), should follow the seasonal trends in otolith edge type quite well. For example, final edge code 1 might be expected to peak in winter, while final edge code 3 might be expected to peak in summer. If these proportions are both sinusoidal, and 180° out of phase, it would be expected that the logit would combine and exaggerate these seasonal trends, yet tame extreme values with the logarithmic transformation (in this paper only natural logarithms were used). Since categories 1 and 3 are mutually exclusive with $p_{1j} + p_{3j} \approx 1$, it would appear that the logit contains most of the information concerning seasonal trend that exists in the data.

We modeled this sinusoidal trend in the (y_j) using $\hat{y}_j = A \times \cos[(2\pi\, j/12) + \phi] + B$ where month $j = 1, \ldots, 12$. The role of the parameters are as follows: A is the amplitude of the seasonal signal, B centers the sinusoidal trend about the observed logits, and ϕ, the phase, describes the time of the year that the logit is expected to peak. If $\phi = 0$, this peak would be in mid-December. If $\phi \neq 0$, then $\hat{y}$ peaks at month $j_{\max} = -12\phi/(2\pi) = -6\phi/\pi$. The values of $j_{\max} = 1, 2, 3...$ can be interpreted as the middle of Jan, Feb, Mar, etc., and the values of $j_{\max} = -1, -2, -3...$ can be interpreted as the middle of Nov, Oct, Sep, etc., because data were collected during the entire month. Since $j_{\max}$ will typically not be an integer, a value such as $j_{\max} = 1.5$ can be interpreted as between January and February (i.e., January 31 or February 1).

The cosine model was fit to the logit data using nonlinear least squares. The parameters $\theta = (A, \phi, B)$ were estimated by minimizing $SS = \Sigma(y_j - \hat{y}_j)^2$. The covariance matrix of $(\hat{A}, \hat{\phi}, \hat{B})$ was estimated using the gradient function $Z = (z_{ij})$ where $z_{ij} = \partial y_i / \partial \theta_j$. The gradient approximation to the covariance matrix is $\Sigma(\hat{A}, \hat{\phi}, \hat{B}) = s^2 (Z'Z)^{-1}$, where $s^2 = SS(\hat{A}, \hat{\phi}, \hat{B})/(n-3)$ and n is the number of months for which a logit was observed that could be used to fit the cosine model. Only months with a minimum of 25 edge-type observations were used in fitting the logit model.

The strength of seasonal variation can be measured by testing the hypothesis $H_0{:}A = 0$, using the t-statistic, $t = \hat{A}/SE(\hat{A})$. Large values of the t-statistic, compared with tabled values of the t-distribution with $n-3$ degrees of freedom would indicate that the strength of the seasonal variation in otolith growth was high. P-values that were provided are for the 2-tailed test. Confidence intervals for the estimated peak of the logit $\hat{j}_{\max} = -6\hat{\phi}/\pi$ can be estimated from $\hat{j}_{\max} \pm t_{0.975,n-3} \times SE(\hat{j}_{\max})$ where $SE(\hat{j}_{\max}) = 6 \times SE(\hat{\phi})/\pi$. This interval for $\hat{j}_{\max}$ can be interpreted as a 95% confidence interval for time at which the logit peak is expected to occur.

RESULTS

The cosine model was fit to the 7 species (Gulf of Alaska and Bering Sea walleye pollock stocks were analyzed separately) for which significant amounts of edge-type data were available (Table 2). The number of otoliths examined varied greatly by species, and depended mostly on the number of specimens that were production aged. Edge interpretations from both whole otoliths and cut-and-burnt otoliths were analyzed together. For most species the predominant ageing method was the cut and burn. However, Atka mackerel otoliths were quite clear, and half of all specimens could be aged from the surface.

Although overall sample sizes were large (Table 2), the sample sizes varied greatly by month and only

Table 2. Parameters estimated from cosine model fit $\{\hat{y}_j = \hat{A} \times \cos[(2\pi\, j/12) + \hat{\phi}]\}$ to logits. For interpretation of parameters see text. N is total sample size, C/B are the number of cut-and-burnt otoliths, n the number of months in the logit fit, and SE are standard errors of parameter estimates. For walleye pollock, Bering Sea (BS) and Gulf of Alaska (GOA) populations were analyzed separately.

Species	N	C/B	n	$\hat{A}$	SE($\hat{A}$)	$\hat{\phi}$	SE($\hat{\phi}$)	$\hat{B}$	SE($\hat{B}$)
Pollock (BS)	54,469	31,744	11	1.775	0.265	-0.855	0.151	0.874	0.189
Pollock (GOA)	44,321	21,057	10	1.377	0.171	-0.779	0.138	0.956	0.128
Sablefish	17,607	14,817	9	0.579	0.065	-1.297	0.111	0.597	0.047
Atka mackerel	14,569	7,552	11	1.101	0.165	-1.305	0.164	0.925	0.122
Pacific ocean perch	7,178	7,173	8	1.385	0.296	-1.666	0.234	0.32	0.236
Northern rockfish	3,403	3,395	7	1.780	0.321	-1.622	0.260	0.873	0.329
Yellowfin sole	13,535	12,518	11	0.749	0.097	-1.009	0.136	1.196	0.070
Northern rocksole	5,544	4,659	10	1.153	0.213	-0.591	0.190	1.099	0.154

months where at least 25 edge-type observations were available were used to fit the logit model. The number of months where sufficient data were available varied from 7 to 11 months. All species that were used in this study had highly significant *t*-statistics indicating that the estimated amplitude of the cosine model, $\hat{A}$, were all significantly different from zero ($\alpha = 0.01$, for the 2-tailed test), and the model fit was not due to chance (Table 3). Also, all 7 species had logits that were consistent with a seasonal (i.e., sinusoidal) progression of edge types with a winter peak in the logit (Figures 4 and 5). The timing of logit peaks (Table 3) varied by species with peaks in pollock and flatfish appearing earlier than peaks in sablefish, Atka mackerel, and rockfish.

Plotting category 1 and category 3 proportions individually can also provide strong evidence of seasonal growth (Figures 4 and 5, right column). All of these plots show the basic seasonal pattern of edge type that would be expected. Category 1 plots are maximal in winter and minimal in summer, while category 3 plots are maximal in summer and minimal in winter. It is interesting to note that all species appear to show their summer maxima (category 3) and summer minima (category 1) in the July–August time period.

Another conclusion that can be drawn from the plot of category 1 and category 3 proportions (Figures 4 and 5, right column) was that the category 2 and category 4 proportions were generally small, since the 4 categories must sum to one. This is why we stated that the quantities "$\log(\hat{p}_{1j} / \hat{p}_{3j})$" are nearly logits.

DISCUSSION

The strength of the logit analysis is that it pools and smoothes the seasonal information on edge-type growth information (Figures 4 and 5), while allowing the use of statistical curve fitting procedures and statistical estimates of logit peaks, and confidence intervals (Tables 2 and 3). Our analysis showed a strong seasonal pattern of the logit peaking in winter and reaching a minimum during the summer.

The simple plots of category 1 and category 3 proportions were also of great value because they clearly indicate which species showed the strongest pattern of seasonal growth. Those species in Figure 4 (pollock, sablefish, and Atka mackerel), where the category proportion actually cross each other in the summer months, seem to show the strongest pattern. The rockfish (Pacific ocean perch and northern rockfish) and flatfish (yellowfin sole, and northern rocksole; Figure 5) also showed fairly strong patterns of seasonal growth, but the category proportions for these species tended to meet at around 0.5 in the summer months rather than actually crossing.

Recording edge types during production age reading is an optional task for age readers. The decision on an edge type is typically subjective. In most cases, readers chose otoliths with unambiguous edge types when recording data. Because younger specimens tend to have less ambiguous edge types, the data are biased towards younger specimens. This could skew the observed timing of the edge categories so they are different from what would be observed in the otoliths of the overall population which includes more old fish.

Although obviously related, the timing of the peak logit ($j_{\max}$) should not be confused with the timing of the deposition of the translucent zone in otoliths. Here, the logit is defined using nearly all of the edge-type data (Table 1), not just data defining the occurrence of the translucent zone. In individual specimens the translucent zone may occur in any month of the year,

Table 3. The statistic *t* measures the significance of the amplitude *A* of the logit cosine model, df is the degrees of freedom of *t*, and the *P*-value is the significance level of the hypothesis test that H_o: $A = 0$. The $\hat{j}_{\max}$ estimates correspond to the month of the peak of the cosine model fit (i.e., the month where category 1 proportions tend to be largest and category 3 proportions tend to be smallest). The $\hat{j}_{\max}$–*low* and $\hat{j}_{\max}$–*high* values are the lower and upper 95% confidence intervals around the peak, using a *t*-statistic with the degrees of freedom shown below. For $\hat{j}_{\max}$ estimates Dec = 0, Jan = 1, Feb = 2, Mar = 3, Apr = 4,…, where fractional values of $\hat{j}_{\max}$ can be interpolated between the month values (see text). For walleye pollock, Bering Sea (BS) and Gulf of Alaska (GOA) populations were analyzed separately.

Species	$t = \hat{A}/SE(\hat{A})$	df = n–3	*P*-value	$\hat{j}_{\max}$	SE($\hat{j}_{\max}$)	$\hat{j}_{\max}$–*low*	$\hat{j}_{\max}$–*high*
Pollock (BS)	6.70	8	0.00015	1.633	0.288	0.968	2.298
Pollock (GOA)	8.05	7	0.00009	1.488	0.264	0.865	2.111
Sablefish	8.91	6	0.00011	2.477	0.212	1.958	2.996
Atka mackerel	6.67	8	0.00016	2.492	0.313	1.770	3.215
Pacific ocean perch	4.68	5	0.00544	3.182	0.447	2.033	4.331
Northern rockfish	5.55	4	0.00517	3.098	0.497	1.719	4.476
Yellowfin sole	7.72	8	0.00006	1.927	0.260	1.328	2.526
Northern rocksole	5.41	7	0.00099	1.129	0.363	0.271	1.987

not just in the winter. In fact it has been observed in many species that older fish appear to lay down their translucent zones later in the year than younger fish.

Beckman and Wilson (1995) examined 104 studies representing 94 species and concluded that the dominant pattern of opaque zone formation in both the northern and southern hemispheres was during spring and summer months. The precise timing and of otolith growth can vary by species, geographic region, age, maturity, depth and many other factors. Therefore, not much can be said that is universal. We only speak to the otoliths of Alaska groundfish, in an effort to verify

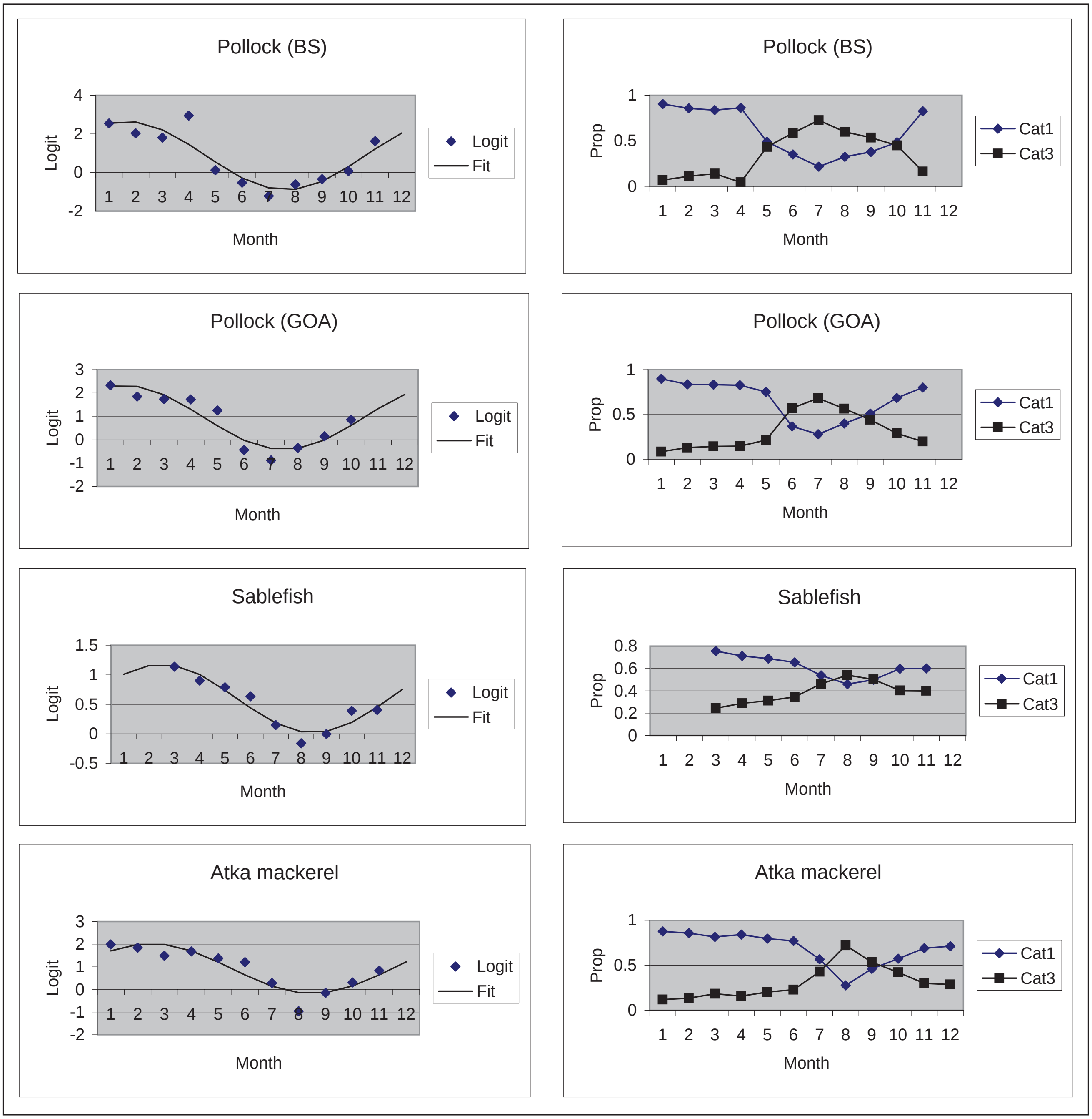

Figure 4. Graphs of logit plots and logit fits to the cosine function (left panels) for 4 groups of groundfish: pollock in the Bering Sea (BS), pollock in the Gulf of Alaska (GOA), sablefish, and Atka mackerel. On the right panels are monthly proportions of final category 1 and final category 3 otolith edge types that comprise the logits on the left. The logit fits on the left only used monthly data supported by at least 25 observations; category data on the right used all data that were available.

that data collected by age readers do in fact contain an annual periodic signal. Results confirm that this is indeed the case.

Despite its shortcomings, marginal increment analysis and the edge type analysis is the most widely applied age validation technique (Cailliet 1990; Campana 2001). However, the subjectivity of edge interpretation, its emphasis on young specimens, and the usual lack of randomization in the experimental design make it an extremely weak form of age validation (Campana 2001; Panfili and Morales-Nin 2002). Campana (2001) carefully describes the weaknesses of marginal increment and edge type analysis and we agree with his conclusion that it is “most likely to be abused.”

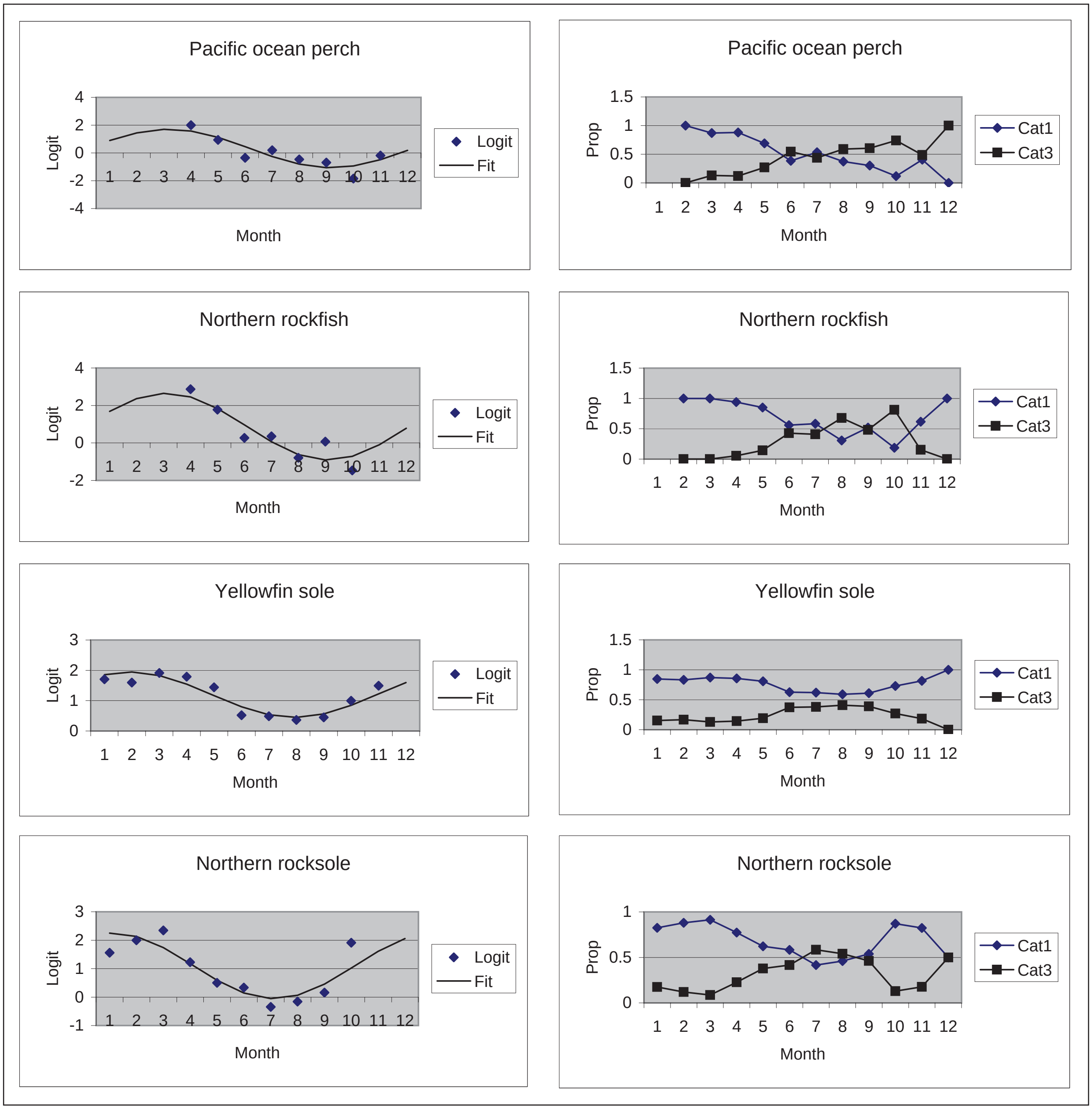

Figure 5. Graphs of logit plots and logit fits to the cosine function (left panels) for 4 groups of groundfish: Pacific ocean perch, northern rockfish, yellowfin sole, and northern rocksole. On the right panels are monthly proportions of final category 1 and final category 3 otolith edge types that comprise the logits on the left. The logit fits on the left only used monthly data where at least 25 observations were available; category data on the right used all data that were available.

We prefer the radiometric (Bennett et al. 1982) and bomb radiocarbon (Kalish 1995) validation methods that are able to validate absolute age, and in the case of bomb radiocarbon it is able to do this with surprising accuracy. In our opinion either known age fish need to be available, or these powerful validation techniques need to be applied for true age validation to occur.

LITERATURE CITED

Beckman, D. W., and C. A. Wilson. 1995. Seasonal timing of opaque zone formation in fish otoliths. Pages 27–43 in D. H. Secor, J. M. Dean, and S. E. Campana, editors. Recent Developments in Fish Otolith Research, University of South Carolina Press, Hilton Head, South Carolina.

Bennett, J. T., G. W. Boehlert, and K. K. Turekian. 1982. Confirmation of longevity in Sebastes diploproa (Pisces: Scorpaenidae) from Pb-210/Ra-226 measurements in otoliths. Marine Biology 71:209–215.

Bishop, Y. M. M., S. E. Fienberg, P. W. Holland, R. J. Light, and F. Mosteller. 1975. Discrete multivariate analysis. MIT Press, Cambridge, Massachusetts.

Cailliet, G. M. 1990. Elasmobranch age validation and verification: an updated review. National Oceanic and Atmospheric Administration Technical Report 90:157–165.

Campana, S. E. 2001. Accuracy, precision and quality control in age determination, including a review of the use and abuse of age validation methods. Journal of Fish Biology 59:197–242.

Chilton, D. E., and R. J. Beamish. 1982. Age determination methods of fishes studied by the Pacific Biological Station. Canadian Special Publication of Fisheries and Aquatic Sciences 60.

Kalish, J. M. 1995. Application of the bomb radiocarbon chronometer to the validation of redfish *Centroberyx affinis* age. Canadian Journal of Fisheries and Aquatic Sciences 52:1399–1405.

Kimura, D. K., and D. A. Anderl. 2005. Quality control of age data at the Alaska Fisheries Science Center. Australian Journal of Marine and Freshwater Research, Special Issue 56:783–789.

Panfili, J., and B. Morales-Nin. 2002. Semi-direct validation. Pages 129–134 *in* J. Panfili, H. de Pontual, H. Troadec, and P. J. Wright, editors. Manual of Fish Sclerochronology, Ifremer, Brest, France.

Pannella, G. 1974. Otolith growth patterns: An aid in age determination in temperate and tropical fishes. Pages 28–39 *in* T. B. Bagenal, editor. The Ageing of Fish. Unwin Brothers, Old Woking, England.